NeuroImage 317 (2025) 121325

Contents lists available at ScienceDirect

NeuroImage

journal homepage: www.elsevier.com/locate/ynimg

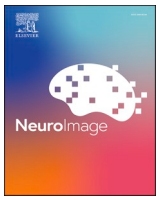

Peripersonal and extrapersonal space encoding in virtual reality: Insights from an fMRI study

Meret Mertens [a,*], Ferdinand Binkofski [a,c,d], Bruno Leitão [b], Bichr Grii [b], Rea Rodriguez-Raecke [b], André Schüppen [a,b], Antonello Pellicano [e], Lukas Lorentz [a,1], Rik Sijben [b,1]

[a] Division of Clinical Cognitive Sciences, Department of Neurology, University Hospital RWTH Aachen, Pauwelsstraße 17, Aachen 52074, Germany
[b] Brain Imaging Facility, Interdisciplinary Centre for Clinical Research, RWTH Aachen University, Germany
[c] Institute for Neuroscience and Medicine (INM-4), Research Center Jülich GmbH, Jülich, Germany
[d] JARA-BRAIN, Jülich-Aachen Research Alliance, Jülich GmbH, Jülich, Germany
[e] Department of Educational Sciences, University of Catania, Catania, Italy

ARTICLE INFO

Keywords:
fMRI
Virtual reality
Peripersonal space
Extrapersonal space
Object processing
Dorsal visual stream
Stereoscopic vision

ABSTRACT

The brain processes objects in reachable peripersonal space and non-reachable extrapersonal space in different neural networks. In contrast to extrapersonal space, spatial processing in peripersonal space is linked to the activation of affordances in dorsal visual pathways. However, the literature on how object characteristics like size, graspability and stereoscopic presentation influence object processing in virtual environments is still unclear.

In the current study, 44 healthy participants performed a visual discrimination task involving graspable objects presented in peripersonal space and extrapersonal space. The paradigm was presented via MRI-compatible goggles during fMRI scanning. The four sessions alternated between monoscopic and stereoscopic presentations and stimuli varied within the sessions in apparent distance, size, and orientation. To validate the effect of distance, the pixel size of objects was also controlled. Stereoscopic presentation enhanced dorsal stream activation, particularly in V5/MT, lateral occipital cortex and the posterior intraparietal sulcus, associated with depth processing, suggesting increased peripersonal space processing. In addition to that, analyses revealed characteristic bilateral activation patterns of primary to tertiary visual areas, extending dorsally from the lateral occipital cortex to the posterior intraparietal sulcus for stimuli in peripersonal space, while extrapersonal space activated mostly ventral regions of the tertiary visual cortex. Notably, as the first study to control for pixel object size, these patterns persist, indicating that stimuli in peripersonal space engage the dorsal visual stream, potentially reflecting action-oriented and grasping feature encoding linked to their interactive affordances, while stimuli in extrapersonal space engage ventral regions primarily mediating semantic aspects and scene analysis.

1. Introduction

The brain's spatial representation is modular, with distinct cortical regions processing peripersonal space (PPS) and extrapersonal space (EPS). These regions guide environmental interactions, survival, and social cognition in primates (Cléry et al., 2015; Rizzolatti et al., 1983) and humans (Basile et al., 2024; Beschin and Robertson, 1997). PPS, a space adjacent to the body's surface, where objects can be reached or manipulated (Brozzoli et al., 2012), is somatotopically organized (Serino et al., 2015; Stone et al., 2018) and dynamic (Farnè and Làdavas, 2000). It integrates multisensory (Serino, 2019) inputs, thereby being essential for the detection of threats (de Borst and de Gelder, 2022; Fossataro et al., 2016; Graziano and Cooke, 2006; Vieira et al., 2020), goal-directed actions (Rizzolatti et al., 1997), and self-perception (Grivaz et al., 2017). EPS, on the other hand, which extends beyond immediate reach, is associated with broader spatial awareness and processed to support long-term planning and navigation (Cléry et al., 2015; Costantini et al., 2011; Previc, 1998).

* Corresponding author.
E-mail address: meret.mertens@rwth-aachen.de (M. Mertens).
[1] These authors contributed equally to this work.

https://doi.org/10.1016/j.neuroimage.2025.121325
Received 11 April 2025; Received in revised form 21 May 2025; Accepted 12 June 2025
Available online 13 June 2025

Neuroimaging studies have identified different neural networks for processing PPS and EPS, reflecting their different functional roles. The PPS network, encompassing parietal and prefrontal regions (Basile et al., 2024), exhibiting plasticity, modulated by the use of tools (Farnè et al., 2005; Farnè and Làdavas, 2000), the presence of social cues (Bogdanova et al., 2021; Heed et al., 2010; Pellencin et al., 2018; Vieira et al., 2020), and emotional states (Cartaud et al., 2018; Ellena et al., 2022; Ruggiero et al., 2017). EPS processing seems to involve other spatial parietal and occipital regions though the underlying mechanisms are not yet fully understood.

Neuronal object processing for PPS and EPS is intrinsically linked to the functional segregation of dorsal and ventral visual pathways. The dorsal and ventral visual pathways, originally referred as the "where" and "what" streams by Mishkin et al. (1983), later associated with action and perception processing (Goodale et al., 1994; Goodale and Milner, 1992) can be further subdivided into more specific substreams. The dorsal pathway includes interconnected, but functionally distinct dorso-, ventro- (Binkofski and Buxbaum, 2013; Rizzolatti and Matelli, 2003) and mediodorsal substreams, (Jüchtern et al., 2024), while there are also latero-ventral and ventro-ventral routes (Pitcher and Ungerleider, 2021; Wurm and Caramazza, 2022). The dorso-dorsal stream, encompassing the superior parietal lobule (SPL) and dorsal premotor areas, primarily facilitates online control of actions (Binkofski and Buxbaum, 2013) due to hidden state exploration, surprise-driven attention and goal-directed motor control (Proietti et al., 2023b). In contrast, the ventro-dorsal stream, which includes the anterior intraparietal sulcus (aIPS), inferior parietal lobule (IPL), and ventral premotor cortex (PMv), is more involved in processing semantic aspects and action comprehension (Binkofski and Buxbaum, 2013; Rizzolatti and Matelli, 2003). This pattern suggests a dorsal-to-ventral gradient, where semantic aspects become increasingly prominent while action-related processing diminishes (Proietti et al., 2023b; Stoll et al., 2024). Therefore, the dorsal visual pathways, primarily engaged in processing stimuli within peripersonal space, play a crucial role in evaluating potential interactions with nearby objects and align with the concept of affordances (Sakreida et al., 2016). In the past Costantini et al. (2011) demonstrated that reaction times were shorter for objects presented in PPS compared to EPS, potentially linked to motor affordances, suggesting that PPS might function as an action space, while EPS processing focuses more on visual and cognitive attributes. However, they did not fully address whether these effects were solely due to spatial distance and action possibilities or influenced by how large the object appears on the retina, which is directly affected by its physical size and proximity to the observer.

The visual system processes object properties hierarchically, with early areas (V1, V2) responding to basic features and higher-order areas (V3) integrating more complex characteristics (Riesenhuber and Poggio, 2000). Depth perception causes far-away objects to appear smaller, while nearby objects appear larger, which may enhance activation in early visual areas (Murray et al., 2006).

Consequently, in the current study, we aimed to address this potential confound by utilizing virtual reality (VR) technology to create a controlled yet realistic environment for presenting graspable objects in both PPS and EPS while controlling the size of an object measured by the number of pixels it occupies in the image (pixel object size). By using a VR headset, we precisely manipulated the apparent distance of objects while maintaining consistent visual angles and maximizing the effect of immersion through stereoscopic presentation. VR systems possess the capacity to generate stereoscopic images, allowing participants to experience depth information in a manner that closely approximates natural perception and therefore enhances the sense of presence (Waldow et al., 2024), a psychological state wherein individuals feel genuinely immersed within the virtual environment (IJsselsteijn et al., 2001). To investigate whether the reaction time effect described by Costantini et al. (2011) could potentially be attributed to the larger proportion of retinal activation caused by greater object size, we analyzed reaction times as well as neuroimaging data.

We hypothesized that, regardless of pixel object size, PPS presentation within reachable distance leads to reduced RT's and preferentially activates dorsal visual stream areas, given its role in processing possible object interactions. To further examine the role of stereoscopic depth cues in the establishment of PPS, we altered the paradigm between monoscopically and stereoscopically presented sessions. We expected to observe further dorsal activations in areas such as the posterior intraparietal sulcus (pIPS), which have been previously associated with three-dimensional (3D) processing and depth cues, based on previous research findings by Durand et al. (2009).

2. Method

2.1. Participants

The final sample consisted of 44 participants with a 1:1 female-to-male ratio and an age range from 19 to 30 ($M = 23.39$, $SD = 2.39$) *years*. One participant had to be excluded from the study due to a coughing fit during the measurement. Participants were recruited via flyers in the University Hospital RWTH Aachen, in university buildings of the FH Aachen, student platforms, as well as on social media between June 2024 and November 2024. The study was advertised to healthy participants between 18–30 years at study onset. Participants were excluded based on the following criteria: past or present neurological or psychiatric disorders, functional magnetic resonance imaging (fMRI) ineligibility (e.g. metal implants, claustrophobia, pregnancy), psychotropic medication use, or a history of drug and alcohol abuse. Each participant received a compensation of 20 € for study participation. The study was approved by the ethics committee (EK 146/22) of the Medical Faculty of RWTH Aachen University. All participants were comprehensively informed about the study, filled in an MRI contraindication checklist, and gave written informed consent in accordance with the Declaration of Helsinki prior to participation.

2.2. Technical setup

The paradigm used in this study was programmed on PsychoPy (Peirce et al., 2019) (version 2024.2.2). Unreal Engine (version 5.2.1, https://www.unrealengine.com) was used to generate stimuli presented in PsychoPy. Following the programming of stimuli in Unreal Engine, these were subsequently incorporated into PsychoPy as static screenshots. This approach was adopted due to the inherent movement restrictions within the MRI environment, which preclude participants from perceiving the broader virtual environment.

While lying in the scanner, the paradigm was presented to the participants via an MRI-compatible goggle system (Visual System HD, NordicNeuroLab, Bergen, Norway), which was attached to the 20-channel head coil. For the right hand, participants received an MRI-compatible button box which they could operate with their right index and middle finger.

2.3. Stimuli description

We presented three cups and three mugs as part of our experimental design. However, the shape and orientation of the objects were not pertinent to our research question. Besides their orientation (upright/inverted) (*see* Fig. 1b), the stimuli were additionally varied in their apparent distance (PPS/EPS) (*see* Fig. 1a), with objects positioned further away generally rendered smaller than those in closer proximity. To control potential confounds arising from this size-distance relationship, object size (large/small) was included as an additional factor in the experimental design (*see* Fig. 1c). This approach ensured that small objects in PPS had equivalent pixel sizes to large objects in EPS (*see* Fig. 1d). By manipulating both distance and size independently, we aimed to examine the individual effects of these variables on neural

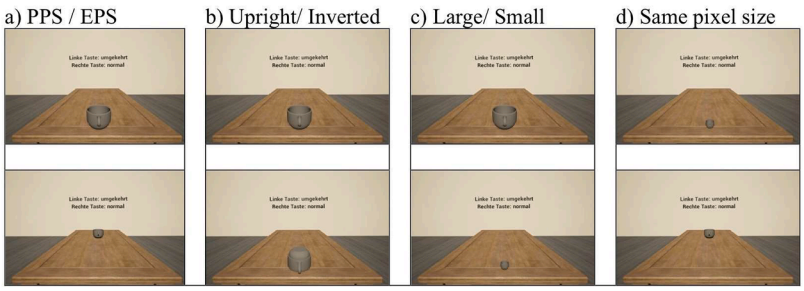

Fig. 1. Representation of the fMRI setup and schematic depiction of experimental timeline. The jittered empty table is followed by the fixation dot as a cue before the cups/mugs are presented. The object presentation included the dynamic decision-making process and the feedback sound, independent of the response time. Description on screen: Linke Taste = left button; Rechte Taste = right button, normal = upright; umgekehrt = inverted.

responses. The combination of the three aforementioned factors created a total of eight experimental conditions (2 × 2 × 2): PPS, upright, small; PPS, upright, large; PPS, inverted, small; PPS, inverted, large, which is the same structure for EPS.

In addition to the eight different conditions within a session, we alternated the binocular disparity of individual sessions between monoscopic and stereoscopic displays to examine whether the stereoscopic, more realistic representation elicited faster or more precise perception.

To account for the distance and field of view (FOV) difference between real life and Unreal Engine's virtual environment settings, a combined scaling factor was calculated from a distance and a FOV scale factor. By using the ratio of average participants' height (175.5 cm) divided by the camera height setting used in unreal engine we calculated a distance scale factor of 0.975. By using the tangent of half the FOV angles (half the FOV corresponds to the angle between the central axis and the edge of the visible area) with a real world FOV of 135° and Unreal Engine FOV of 90°, we calculated a FOV scale factor of 0.414. Multiplying these two factors produced a combining scaling factor of 0.404, which was then applied to the PPS and EPS distances measured through unreal engine's measuring tool to confirm the real-life distance. To maintain consistency across participants, a standardized distance for PPS and EPS was used rather than determining individualized peripersonal distances. The virtual PPS distance of 136 cm was scaled to 54.9 cm in real life, which, in turn, falls within the range of 50 ± 14 cm, which has been described by Costantini et al. (2011) as PPS distance, meanwhile the virtual EPS distance of 311 cm was scaled to approximately 125.53 cm in real life. This ensures that the participants perceive the cups in the intended PPS or EPS distance respectively. Additionally, participants were asked to rate their sense of immersion in the virtual scenario from zero to ten and the perceived graspability of objects at varying distances with yes or no after each session to further confirm that nearby objects were perceived as being situated in the participants' individual PPS.

2.4. Paradigm description

In the virtual scenario, participants were situated in an environment featuring a large, empty dining table positioned centrally in front of them. This spatial arrangement was designed to create the perspective of sitting directly at the table. In the background of the experimental setting, a prominent inscription was displayed on the wall. This inscription served to reiterate the task instructions, ensuring that participants had a visual reference to consult in case they forgot which button to press during the task (*see* Fig. 2). Throughout the entire experiment, the participants' task was to indicate as quickly as possible whether they detected the presented stimuli (cups/mugs) as inverted or upright by pressing either the left button with their index finger for "inverted" or the right button with their middle finger for "upright". Upon selecting the response on the keyboard, participants immediately received auditory feedback during the presentation of the stimulus. A correct answer was signaled by a high-pitched sound (660 Hz), while an incorrect or missing answer was indicated by a low-pitched sound (330 Hz), using Optoactive II noise cancelling headphones from Opto-Acoustics (https://www.optoacoustics.com/medical/optoactive-ii0).

At the beginning of each trial, participants were first presented with an empty table for a duration jittered and pseudorandomized between 4500 and 5500 ms, followed by a fixation dot displayed at the center of the maximum distance of the stimuli for 500 ms. Subsequently, the stimulus was presented for 2300 ms, independent of the participants' response times, to ensure that the duration of the stimulus event was consistent across all trials (see Fig. 2).

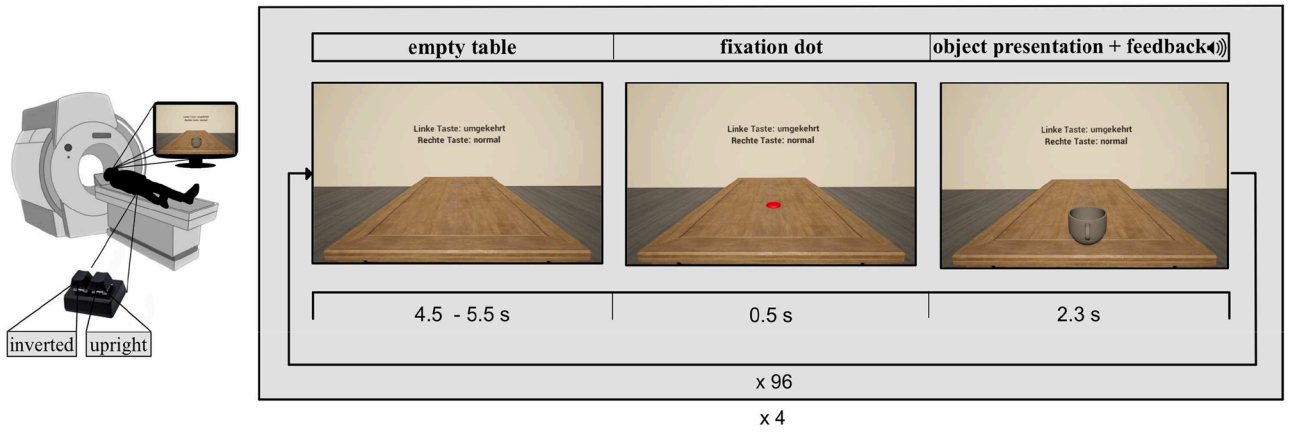

Fig. 2. Representation of different stimuli condition. The cups/mugs varied in a) distance (PPS = peripersonal space /EPS = extrapersonal space) b) orientation (upright/inverted) and c) size (large/small). d) PPS_small and EPS_large cups/mugs displayed same pixel size on the retina.

2.5. Procedure

Data acquisition was conducted at the University Hospital Aachen (Germany). The attending researcher led participants to the examination room, providing instructions for the in-scanner task and inter-session questionnaire. Following removal of all metallic objects, participants were positioned in the MRI scanner, where an MRI-compatible goggle system was attached to the head coil and adjusted for interpupillary distance and optical diopter using a stereoscopic test image when necessary. Inflatable cushions were provided for head stabilization within the coil. To minimize head motion, a strip of surgical tape was applied to participants' foreheads, serving as a proprioceptive cue. Once participants were equipped with the response button box and familiarized with its operation, the experimental protocol was initiated.

In total participants completed four experimental sessions, each lasting 12 min and 52 s, which alternately varied counterbalanced in their binocular disparity between monoscopic and stereoscopic presentation. Each session consisted of 96 trials, as each of the 8 conditions (2 × 2 × 2) was presented 12 times in pseudorandomized order. Structural images were obtained between sessions two and three, allowing participants to have a resting phase around six minutes. At the beginning of the experiment, a localizer sequence and gradient-echo field map were acquired.

2.6. Behavioral analysis

All analyses were performed using MATLAB (version 2020b, MathWorks, Natick, MA, USA) and SPSS (IBM SPSS Statistics 20.0, Chicago, IL, USA). A repeated measures ANOVA was conducted to examine the effect of four independent variables: distance, orientation, size and binocular disparity on the response time of participants. The dependent variable, response time, was measured in milliseconds. For the repeated-measures ANOVA, trials within the same condition were averaged to derive a single value for each condition per participant.

In addition to the main effects, we examined two-way and three-way interactions.

Prior to conducting the ANOVA, normality was verified with Kolmogorov-Smirnov test. Despite potential violations of normality in three out of 16 conditions the use of parametric tests remains justifiable. The robustness of ANOVA to moderate deviations from normality, particularly in the absence of obvious outliers, coupled with its balanced design and sufficient sample size, supports the validity of the analysis (Blanca et al., 2017; Schmider et al., 2010). For all analyses, a significance threshold of $\alpha = 0.05$ (two-tailed) was used. Post-hoc analyses were corrected for multiple comparisons using the Bonferroni method.

2.7. Functional MRI data analysis

2.7.1. Scanning procedure

All images were acquired on a Siemens Prisma 3-Tesla scanner (Erlangen, Germany) using a 20-channel head coil. Structural images were obtained using a T1-weighted magnetization-prepared gradient-echo sequence (MPRAGE; TR = 2300 ms, TE = 2.32 ms, TA = 5.35 min, flip angle = 8°, FOV = 240 mm x 240 mm, acquisition matrix = 256 × 256, slices = 192, interleaved, voxel size = 0.9375 mm x 0.9375 mm, slice thickness = 0.9 mm. A T2*-weighted echo-planar imaging (EPI) sequence (TR = 1560 ms, TE = 37 ms, multi-band acceleration factor = 3, flip angle = 72°, FOV = 220 mm x 220 mm, acquisition matrix = 88 × 88, slices = 60, interleaved, voxel size = 2.5 × 2.5 × 2.5 mm) was used for the acquisition of the functional blood-oxygen-level-dependent (BOLD) images. The sequence covered the whole brain and slices were positioned transaxially, parallel to the anterior–posterior commissural line, using a localizer sequence at the beginning of each measurement. A gradient-echo field map was acquired with the following parameters: TR = 438 ms, short TE = 4.92 ms, long TE = 7.38, TA = ~ 1 min, flip angle = 60°, FOV = 228 mm x 228 mm, acquisition matrix = 76 × 76, slices = 45, voxel size = 3 × 3 × 3 mm.

2.7.2. Preprocessing

Functional images were preprocessed and analyzed with the Statistical Parametric Mapping software (SPM12 software, http://www.fil.ion.ucl.ac.uk/spm/) launched on MATLAB R2020b (MathWorks, Natick, MA, USA). Initially, a voxel displacement map was generated utilizing gradient-echo sequences alongside the standard brain mask image from SPM. To correct for distortion effects in the EPI scans, the precalculated phase map was subsequently applied to the EPI scans during the distortion correction phase of the realignment process. The unwarped EPI scans were then realigned to the first volume, which served as a reference. Each individual anatomical scan was co-registered with the mean EPI scan of the corresponding session to facilitate accurate overlay and segmentation for subsequent analyses. Tissue probability maps from SPM were used to normalize the anatomy and EPI scans to Montreal Neurological Institute (MNI) 152 standard space. Lastly, the EPI scans were smoothed using an 8-mm full-width-at half-maximum Gaussian kernel to improve signal-to-noise ratio.

2.7.3. Single-subject analysis

Once preprocessing was completed, we implemented a general linear model approach in SPM to perform first-level analyses on individual subject data. The experiment consisted of four sessions, each comprising eight conditions out of three factors each (distance, orientation, size). The sessions alternated within an additional factor (monoscopic/stereoscopic). Therefore, we constructed design matrices incorporating sixteen task-related regressors per session corresponding to the onset of the visual stimulus based on our experimental paradigm. Another regressor of no interest was included for the fixation dot. All stimuli were modeled as events. The stimulus onset function was convolved with a canonical hemodynamic response function to model expected brain activity associated with each task condition. In addition, the six realignment parameters were added to capture residual movement-related artifacts. Sixteen main contrasts were constructed on the first level for subject-wise analysis, each representing a unique combination of all four factors (2 × 2 × 2 × 2) mentioned above.

2.7.4. Group analysis

To allow for population inference, simple contrasts were elevated to the second level and used to recreate the complex contrasts using a within-subject ANOVA. Eight t-contrasts of interest were included in the final analysis. To investigate the hypothesis that regions associated with the PPS network would be activated during presentations in PPS, and areas of the EPS network during presentations in EPS, irrespective of stimulus size, with potentially enhanced activations under stereoscopic conditions, we contrasted the main effect between PPS and EPS in both [PPS > EPS] and [EPS > PPS] directions, stereoscopic presentation (ST) and monoscopic presentation (M) in both [ST > *M*] and [*M* > ST] directions, and small (S) and large (L) objects in both [*S* > *L*] and [*L* > *S*] directions. Another specific t-contrast assessing the effect of distance, controlled for object size (both objects had same pixel size: peripersonal_small, extrapersonal_big) was analyzed in both [PPS_*S* > EPS_B] and [EPS_*B* > PPS_S] directions to explicitly control for the influence of size. All reported results passed the family-wise-error (FWE) corrected significance threshold of $p < .05$ on the voxel level, with exception of the statistical map of the [ST ⟩ M] contrast. To investigate whether a lower, FWE corrected, threshold, could reveal symmetric activations following our initial observation of unilateral activations only, this contrast was thresholded at a voxel level of $p < .001$ and a cluster-fewel FWE correction < 0.05 (cluster extent threshold > 159 voxels).

3. Results

3.1. Behavioral results

The repeated measures ANOVA of the behavioral data indicated that objects in EPS elicited significant longer response times compared to those in participants' PPS ($M_{PPS} = 0.769$, standard error (SE) = 0.022; $M_{EPS} = 0.818$, $SE = 0.023$; F (1,43) = 77.55, $p < .001$, $\eta_p^2 = 0.643$) (*see* Fig. 3a). In addition to that, small objects resulted in significant longer response times than large objects ($M_S = 0.833$, $SE = 0.022$; $M_L = 0.754$, $SE = 0.023$; F (1,43) = 214.64, $p < .001$, $\eta_p^2 = 0.833$) (*see* Fig. 3a). Post-hoc comparisons using the Bonferroni correction confirmed these significant differences.

Furthermore, significant interaction effects between distance and size (F (1,43) = 15.38, $p < .001$, $\eta_p^2 = 0.263$) were found. Specifically, size exhibited a significant effect at both levels of distance, and distance demonstrated a significant effect at both levels of size. However, the mean difference of size in EPS ($M_{EPS\_S} = 0.865$, $SE = 0.024$, $M_{EPS\text{-}L} = 0.771$, $SE = 0.023$) was slightly larger than in PPS ($M_{PPS\_S} = 0.801$, $SE = 0.022$, $M_{PPS\_L} = 0.737$, $SE = 0.023$) (*see* Fig. 3b). For size, a slightly more pronounced effect was detected for small objects ($M_{PPS\_S} = 0.801$, $SE = 0.022$, $M_{EPS\_S} = 0.865$, $SE = 0.024$) compared to large objects in PPS and EPS ($M_{PPS\_L} = 0.737$, $SE = 0.023$, $M_{EPS\text{-}L} = 0.771$, $SE = 0.023$) (*see* Fig. 3b).

Important to highlight is, that participants demonstrated significantly shorter response times ($t = 4.75$, $p < .001$, $d = 0.716$) for large, EPS objects ($M_{EPS\text{-}L} = 0.771$, $SE = 0.023$) compared to small, PPS objects ($M_{PPS\_S} = 0.801$, $SE = 0.022$) that possessed the same pixel size (*see* Fig. 3b).

Additionally, significant interaction effects were observed between orientation and size (F (1, 43) = 5.63, $p = .022$, $\eta_p^2 = 0.116$) and distance and binocular disparity (F (1, 43) = 5.20, $p = .028$, $\eta_p^2 = 0.108$). Although the interaction effect between size and orientation was significant, the simple effects did not reach significance (*see* Fig. 3c). For the interaction between distance and binocular disparity, binocular disparity yielded an effect in EPS with shorter response times in monoscopic presentation ($M_{EPS\_M} = 0.808$, $SE = 0.024$, $M_{EPS\text{-}ST} = 0.828$, $SE = 0.024$). In the PPS, however, this effect was not significant (*see* Fig. 3d).

While no statistically significant effects were observed for orientation ($p = .62$) or any other interactions of the independent variables ($p > .05$), the effect of binocular disparity approached significance ($p = .073$).

3.2. Questionnaire results

The level of immersion reported by participants within the virtual environment ranged from two to ten ($M = 6.09$, $SD = 1.85$). A direct comparison of the sense of immersion ratings between monoscopic and stereoscopic sessions showed that stereoscopic presentation ($M = 6.22$, $SD = 1.77$) was associated with significantly stronger feelings of presence ($t = 2.77$, $p = .008$) than monoscopic presentation ($M = 5.97$, $SD = 1.927$).

All participants, except one, confirmed that objects presented within PPS would have been graspable without altering their position. Correspondingly, all participants, except one, indicated that objects presented at a greater distance were not graspable. These results validate the effectiveness of our experimental design in distinguishing between presentations in PPS and EPS.

3.3. fMRI results

To evaluate the main effects of distance [PPS > EPS], [EPS > PPS], size [$S > B$], [$B > S$] and binocular disparity [ST > M] on the whole brain level, complex contrasts were calculated by means of a within-subject ANOVA (*see* Table 1). No significant activations were observed in the [M > ST] contrast.

Contrasting presentation in PPS and EPS revealed distinct patterns of neural activation. Presentation in PPS elicited increased activity in bilateral central regions of visual areas V1, V2, V3v, V3A, V3d, the

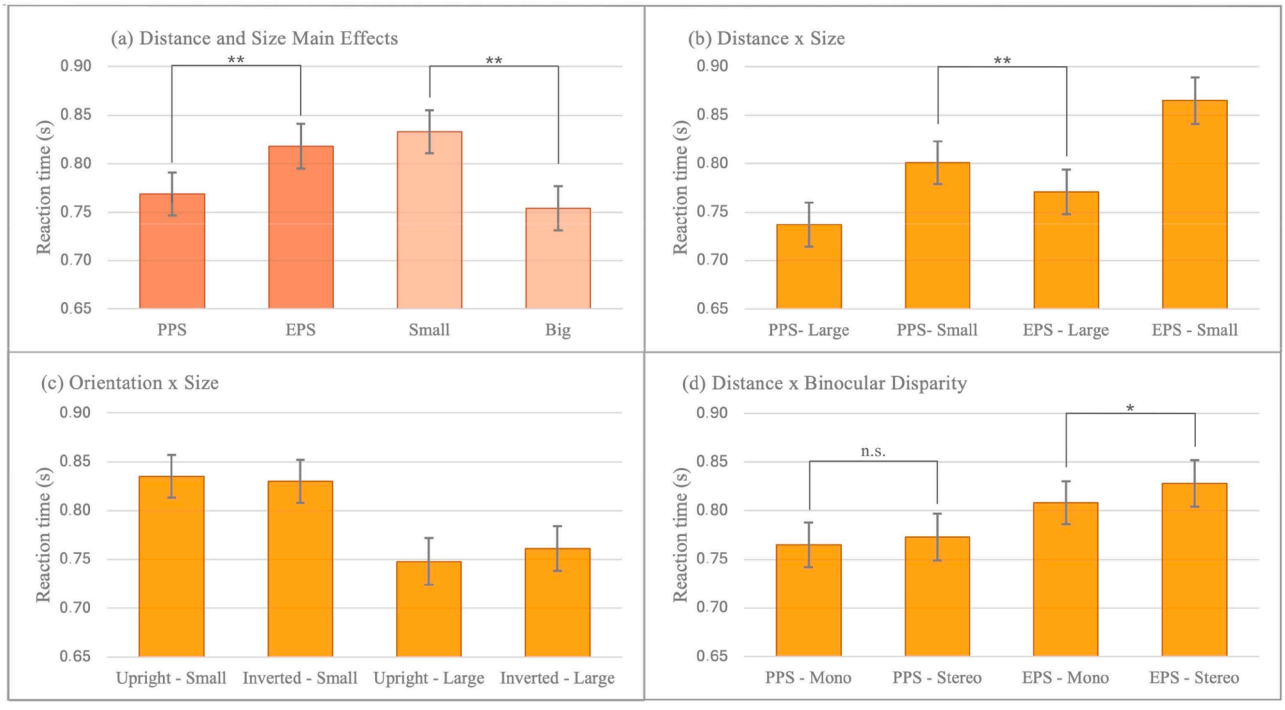

Fig. 3. Bar charts depicting mean response times (±SE) for (a) distance and size main effects. Additional bar charts illustrate mean response times (± SE) demonstrating interaction effects between (b) distance and size, (c) orientation and size, and (d) distance and binocular disparity. Significant differences are represented with asterisks: * $p < .05$, ** $p < .001$, n.s. = not significant. PPS = peripersonal space, EPS = extrapersonal space, Mono = monoscopic, Stereo = stereoscopic.

Table 1
fMRI results showing the results of the main contrasts (binocular disparity, size and distance).

Main contrast	k	Region	H	MNI (x,y,z)			t
Binocular disparity [Stereoscopic > Monoscopic] *	159	Visual Area 5 / MT	R	+46	- 67	+5	5.31
	163	Visual Area 5 / MT	L	-44	-74	+2	4.57
		Area hOc4Ia/ LOC	L	-40	-84	+10	3.43
	253	Intra-Parietal Sulcus	R	+23	-77	+20	4.33
		Intra-Parietal Sulcus	R	+28	-82	+22	4.07
		Intra-Parietal Sulcus	R	+26	-72	+28	4.05
Distance [PPS > EPS]	4462	Visual Area 2	R	+13	-74	-2	18.90
		Visual Area 3d	R	+20	-92	+20	17.40
		Visual Area 2	R	+13	-94	+15	17.10
		Visual Area 3a	L	-14	-94	+18	16.40
		Visual Area 2	L	-10	-100	+12	15.60
		Visual Area 3v	L	-7	-80	-5	15.40
		Visual Area 1	R	+10	-62	+2	12.30
		Visual Area 1	L	-10	-62	+0	12.00
		Visual Area 2	R	+20	-54	-8	9.62
		Visual Area 1	L	-20	-57	-5	8.32
Distance [EPS > PPS]	405	Visual Area 3v	R	+30	-94	-8	21.60
	285	Visual area 3v	L	-27	-97	-10	20.80
	264	Visual Area 3d	R	+6	-77	+20	10.30
Size [Small > Large]	261	Area hOc4Ip/ LOC	L	-27	-100	-8	23.00
	310	Area hOc4Ip/ LOC	R	+28	-97	-5	22.70
	897	Area 6mr/ preSMA	R	+8	+10	+52	8.04
		Area 6mr/ preSMA	L	-10	+18	+38	5.29
	1267	Area 44	R	+48	+8	+28	7.92
		Area OP 9/ Operculum	R	+33	+23	+10	7.24
		Area 4a	R	+38	-4	+50	6.25
		Area 45	R	+43	+36	+15	5.22
	318	Area Id7/ Insular Cortex	L	-30	+23	+5	6.92
	146	Cerebellum, Vermis IV	L	-4	-74	-22	6.26
		Cerebellum, VI	R	+8	-70	-22	5.78
	123	Visual Area 2	L	-14	-70	+8	6.18
		Visual Area 1	L	-12	-62	+0	5.54
	255	Precentral Gyrus	L	-40	-12	+52	6.15
		Area 44	L	-47	+3	+32	5.55
	137	Visual Area 1	R	+13	-62	+2	5.99
	25	Cerebellum, Left VI	L	-27	-62	-28	5.37
	176	Intra-Parietal Sulcus	R	+13	-72	+40	5.33
		Intra-Parietal Sulcus	R	+30	-64	+30	5.26
		Intra-Parietal Sulcus	R	+30	-50	+40	5.22
		Intra-Parietal Sulcus	R	+20	-60	+32	4.79
		Intra-Parietal Sulcus	R	+23	-57	+30	4.77
	33	Cingulate Gyrus, anterior	L	-4	+28	+28	5.11
	28	Cingulate Gyrus, posterior	R	+6	-24	+28	5.05
Size [Large> Small]	426	Visual Area 4v	R	+23	-80	-8	15.50
	1758	Visual area 3d	R	+20	-92	+18	14.50
		Visual Area 3a	L	-14	-94	+20	13.30
		Area hOc4Ia/ LOC	L	-42	-82	+2	6.72
	392	Visual Area 4v	L	-22	-80	-8	14.50
	39	Area hOc4Ia/ LOC	R	+46	-80	+5	5.41

Note: H = Hemisphere, MNI = Montreal Neurological Institute, *t* = *t*-test statistical value, *k* = cluster size, *L* = left, *R* = right, PPS = peripersonal space, EPS = extrapersonal space, LOC = Lateral Occipital Cortex, MT = Middle Temporal Visual Area, SMA = Supplementary Motor Area.

* All results are significant at $p < .05$ corrected for family-wise error (FWE) at voxel-level and a voxel extent threshold of $k \geq 20$ with the exception of the [ST > *M*] contrast which was significant at $p < .001$ for family-wise error (FWE) at cluster-level correction ($k \geq 159$). Anatomical labeling was performed using the Anatomy Toolbox (version 3.0) within SPM.

lateral occipital cortex (LOC), and the IPS whereas presentation in EPS was associated with increased activity in bilateral lateral regions of V3v and a central activation cluster in V3d (*see* Fig. 4a, b *and* Table 1).

Results of the contrast between small more than large stimuli show significant bilateral activation in the primary visual areas V1 and V2, the LOC and the IPS. Bilateral activation clusters were also observed in prefrontal regions, including the pre-supplementary motor area (pre-SMA), Brodmann areas 44, 45 (BA 44/45), and 4a (BA 4a), as well as the operculum, anterior and posterior cingulate cortex (ACC/PCC), cerebellum, and anterior insular cortex (see Fig. 4d and Table 1). As illustrated in Fig. 4c and Table 1, large stimuli in contrast demonstrated pronounced activations in bilateral visual areas V3d, V3A, and V4v and parts of the LOC.

As illustrated in Fig. 4e *and* Table 1, stereoscopic presentation compared to monoscopic presentation of the attention task induced several clusters of significantly increased activation including different regions in both the dorsal and ventral visual streams. As part of the ventral visual processing stream, certain regions of the LOC were activated. Additionally, bilateral V5/MT and the IPS of the dorsal stream exhibit increased activation.

3.4. Specific contrast of distance controlled for static pixel size

As illustrated in Fig. 5 *and* Table 2, changes in distance, independent of pixel object size induced several different clusters of significantly increased activation.

Representation in PPS elicited activations in bilateral visual areas V1, V2, V3v, V3d, and the IPS, whereas the representation of objects with identical pixel size in EPS induced activations in bilateral visual areas V2 and V4v.

4. Discussion

The present study aimed to investigate the neural processing of object presentation in PPS and EPS while controlling for pixel object size, using realistic and graspable objects presented through VR in alternated monoscopic and stereoscopic sessions.

Our neuroimaging results demonstrate that stimuli in PPS activate bilateral primary (V1, V2) and higher-order visual regions (V3A, v, d) as well as the CIP as part of the pIPS (*see* Fig. 4a). Enhanced depth cues and action-related processing of objects in PPS lead towards the

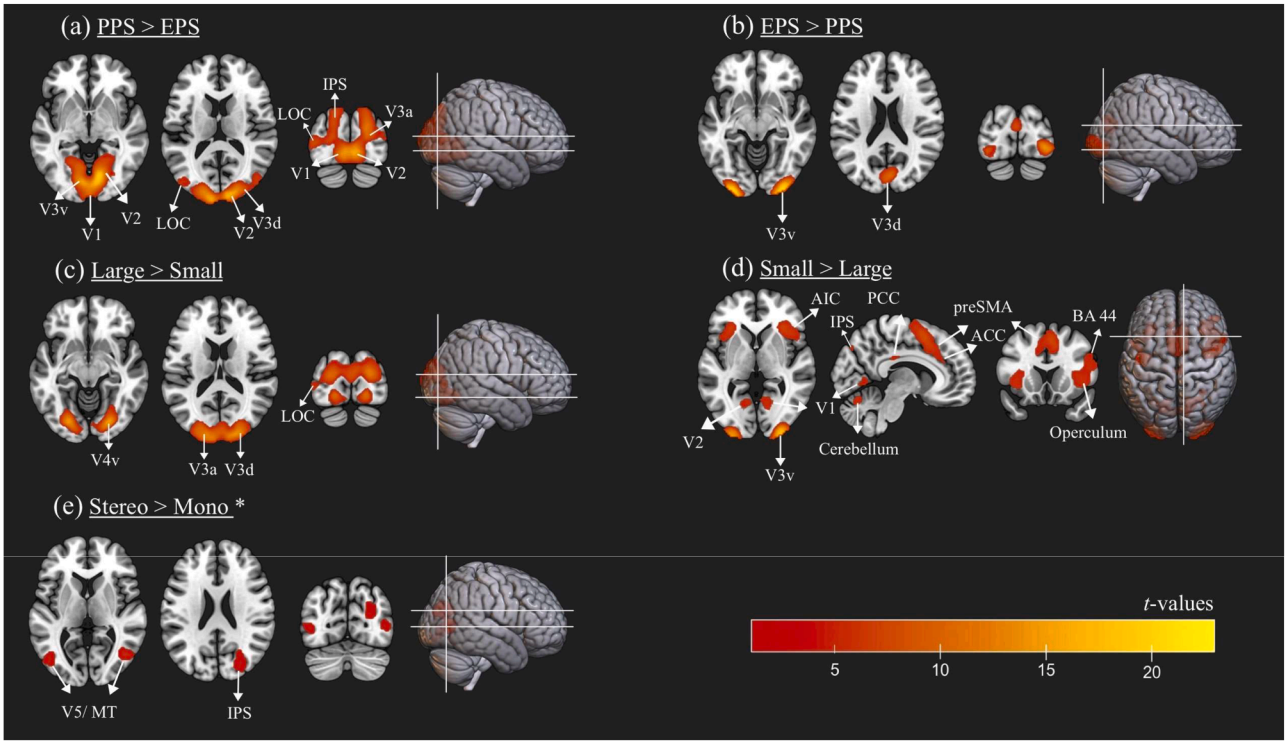

Fig. 4. Areas of significant BOLD increase for contrasts a)/b) PPS = peripersonal space >/< EPS = extrapersonal space; c)/d) Large >/< Small; e) Stereo > Mono. The statistical threshold map is set to $p < .05$, family-wise error corrected at voxel level for (a), (b), (c) and (d). * = for (e) the statistical threshold map is set to $p < .001$ at voxel level and $p < .5$ FWE corrected at cluster level. The figure was created with MRIcroGL1.2. software. V1 = Primary Visual Cortex; V2 = Secondary Visual Cortex; V3A = Tertiary Visual Cortex A; V3V = Ventral Tertiary Visual Cortex; V3D = Dorsal Tertiary Visual Cortex; V4 = Quaternary Visual Cortex; V5/MT = Quinary Visual Cortex/Middle Temporal Visual Area; BA 44 = Brodmann Areal 44; IPS = Intraparietal Sulcus; LOC = Lateral Occipital Cortex; SMA = Supplementary Motor Area; ACC = Anterior Cingulate Cortex; PCC = Posterior Cingulate Cortex; AIC = Anterior Insular Cortex.

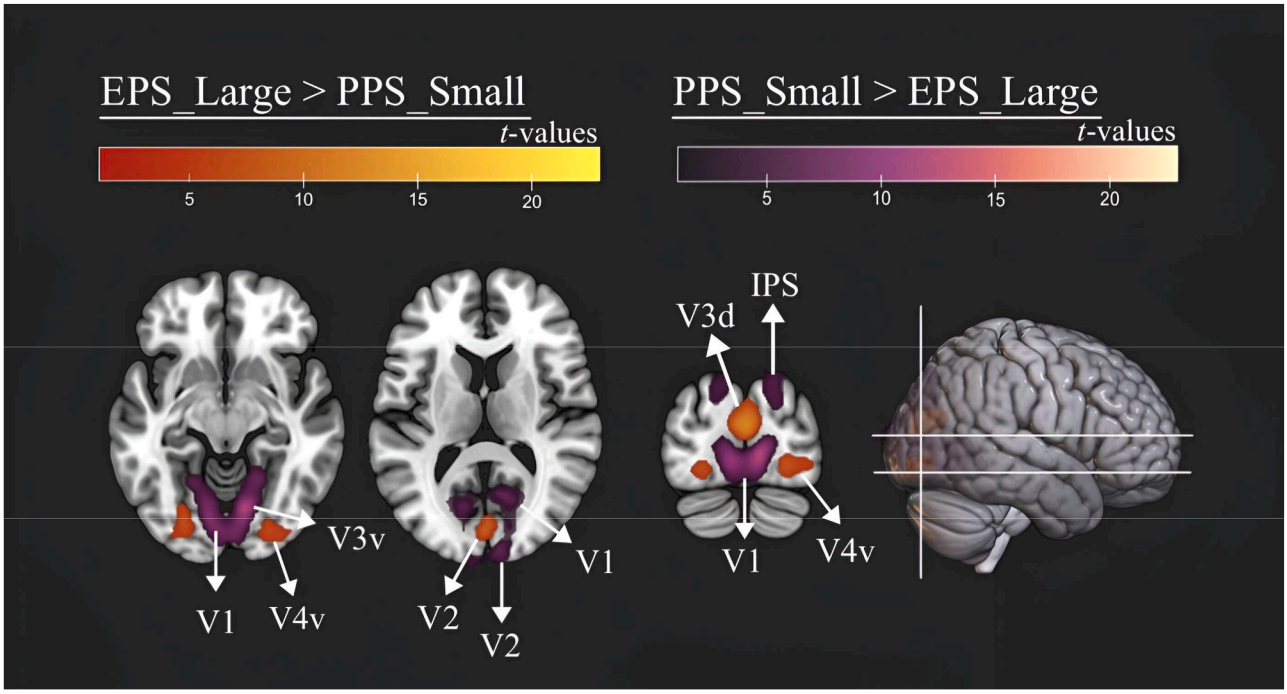

Fig. 5. Areas of significant BOLD increase for Extrapersonal space_Large >/< Peripersonal space_Small. The statistical threshold map is set to $p < .05$, family-wise error corrected at voxel level. The figure was created with MRIcroGL1.2. software. EPS = Extrapersonal space; PPS = Peripersonal space; V1 = Primary Visual Cortex; V2 = Secondary Visual Cortex; V3V = Ventral Tertiary Visual Cortex; V3D = Dorsal Tertiary Visual Cortex; V4V = Quaternary Visual Cortex V; IPS = Intraparietal Sulcus.

Table 2
fMRI results showing the results of the specific contrast (combination of distance and static pixel size).

Specific contrast	k	Region	H	MNI (x,y,z)			t
Same pixel size [PPS_Small > EPS_Large]	2547	Visual area 3v	R	+13	-72	-2	18.70
		Visual area 1	R	+10	-62	+2	14.30
		Visual area 1	L	-10	-62	+0	13.90
		Visual area 3v	L	-10	-77	-5	12.50
		Visual area 1	L	-2	-102	+5	7.15
		Intra-Parietal Sulcus	R	+20	-80	+42	6.91
		Intra-Parietal Sulcus	R	+18	-80	+38	6.86
		Visual Area 2	L	-10	-102	+15	5.41
		Visual Area 3d	R	+20	-92	+20	4.99
	426	Intra-Parietal Sulcus	L	-14	-82	+38	6.01
Same pixel size [EPS_Large > PPS_Small]	378	Visual area 2	R	+3	-82	+18	12.80
	133	Visual Area 4v	L	-24	-74	-5	8.59
	146	Visual Area 4v	R	+26	-82	-5	8.50

Note: H = Hemisphere, MNI = Montreal Neurological Institute, t = t-test statistical value, k = cluster size, L = left, R = right, PPS = peripersonal space, EPS = extrapersonal space, LOC = Lateral Occipital Cortex. * All results are significant at $p < .05$ corrected for FWE at voxel-level ($k \geq 20$). Anatomical labeling was performed using the Anatomy Toolbox (version 3.0) within SPM.

mediodorsal, "movement coordination and object manipulation"-pathway (Jüchtern et al., 2024), whereas stimuli in EPS primarily activate the higher visual areas V3 (V3v, V3d), extending a more ventral pathway involved in processing semantic representations and action comprehension (Binkofski and Buxbaum, 2013; Rizzolatti and Matelli, 2003) (*see* Fig. 4b). Specifically, objects in PPS are perceived as directly interactable, enabling actions such as grasping or manipulating and therefore being associated with the concept of affordances, processed through the dorsal visual streams (Sakreida et al., 2016). By controlling for pixel object size, we ensured that any activations (e.g., V1, V2, V3, IPS) were not solely attributable to stimulus size on the retina but reflect spatial processing differences between peripersonal and extrapersonal space (*see* Fig. 5).

Stereoscopic presentation enhanced activations across diverse cortical regions, such as the pIPS, V5/MT and the LOC, known to be implicated in depth perception and 3D shape processing (*see* Fig. 4e). This increased neural activity demands additional cognitive resources, potentially leading to longer response times during tasks requiring spatial judgments or interactions.

4.1. Behavioral findings

As anticipated, participants exhibited shorter response times for closer and larger objects (*see* Fig. 3a) aligning with significant biological relevance (e.g., fight/flight, go/no-go) (Horváth et al., 2018). Enhanced depth cues, due to local contrasts, depth of field, and ambient occlusion, facilitated quicker processing of larger objects (Rößing et al., 2012). Notably, large objects in EPS elicited faster responses than small ones in PPS of equal pixel size (*see* Fig. 3b), suggesting the visual system integrates depth and spatial context to perceive the object in EPS as larger and leading to shorter response times aligning with Plewan et al. (2012).

Our results also revealed a significant interaction between object distance and size (*see* Fig. 3b), consistent with decades of research on their mutual influence on perception (Chen et al., 2020; Gruber, 1954; Higashiyama and Shimono, 2004; Holway and Boring, 1941; Kilpatrick and Ittelson, 1953). Size effects were more pronounced in EPS, due to increased task difficulty at greater distances. While objects in PPS are easily recognizable regardless of size, smaller objects in EPS are more challenging to identify thereby potentially leading to increased reaction times (Gori et al., 2011).

Of greater interest is also the significant effect of binocular disparity in EPS. Stereoscopic representation enhances depth attributes and immersion, potentially increasing processing complexity (Cho et al., 2016) and leading to slower response times when discriminating between upright and inverted objects in EPS (*see* Fig. 3d). Moreover, stereoscopic presentation may appear more distant and harder to identify in EPS matching with McIntire et al. (2012). The enhanced perceptibility of cups in PPS aligns with findings that suggest that stereoscopic presentation offers minimal further three-dimensional perception in simple tasks where alternative depth cues are readily available and depth information is not critical for optimal performance (McIntire et al., 2012). The distance perception questionnaire results validated our effective manipulation of PPS and EPS in the experimental design.

The interaction between orientation and size (*see* Fig. 3c) was of limited relevance for further analysis and its influence on PPS and EPS.

4.2. fMRI findings

4.2.1. PPS and EPS processing

The processing of stimuli in PPS engages both bilateral primary and higher visual areas of the occipital and temporal cortex, like V1, V2, and V3 (a, d, v), as well as the pIPS (see Fig. 4a and Table 1). Conversely, the representation of stimuli in EPS primarily leads to bilateral activations in occipital visual area V3 (v, d) (see Fig. 4b and Table 1).

The level of activation in early visual areas such as V1 and its downstream area V2 is influenced by the distance of the stimulus, with closer objects, which appear larger, typically evoke stronger responses (Murray et al., 2006; Anderson and Martin, 2009).

However, these activations are not solely determined by pixel size but are modulated by contextual factors and 3D scene content aligning with Fang et al. (2008), Murray et al. (2006) and Sperandio et al. (2012). Our results showed significant V1 and V2 activations for stimuli in PPS, even when corrected for pixel size, exhibiting more detail and enhancing depth information (Blini et al., 2018) due to altered viewing angles, resulting in a top-down perspective that accentuated 3D properties (see Fig. 1).

Enhanced 3D properties of objects in PPS increase activation not only in early visual areas V1 and V2 but also in the higher visual area V3A, regarding the essential role of V3A in encoding depth cues for perceiving 3D space in humans (Chen et al., 2020; Lorentz et al., 2023). Conversely, stimuli in EPS, viewed from a straight, direct angle provide fewer visual cues for depth and 3D shape (see Fig. 1).

Alongside V3A activation, significant activations were observed in other higher visual areas V3d and V3v (see Fig. 4a, b and Table 1), which are known to form complementary representations of upper and lower visual quadrants (Gattass et al., 1988), with V3d potentially containing a central "gap" for upper visual field processing (Kaas et al., 2015). Distant stimuli positioned in the upper visual field activate the central "gap" of V3d, while stimuli in PPS positioned in the lower visual field activate lateral regions of V3d, supported by our results. Considering the findings by Berryhill and Olson (2009) suggesting that V3d is also implicated in perceived distance processing, it can be assumed that V3d plays a role in encoding distance by integrating information about an object's position within the visual field. In contrast, V3v plays a key role in recalculating perceived object size based on distance (Weidner et al., 2014). Objects in PPS activated central V3v regions, processing detailed visual information of nearby objects, while objects in EPS activated lateral V3v regions,

handling distant object representations (*see* Fig. 4 a, b). This aligns with findings from Malach et al. (2002), that fine detail analysis occurs in central, "high-magnification" areas, while large-scale integration happens in peripheral, "low-magnification" regions.

In addition to activations in visual areas, our study revealed significant activations in the posterior IPS/ hIP7, which is considered homologous to the caudal intraparietal area (CIP) in macaque monkeys (Orban and Ferri, 2016; Shikata et al., 2008), in response to stimuli in PPS (see Fig. 4a). Previous research has mentioned the IPS as a key component of the PPS brain network (Basile et al., 2024; Cléry et al., 2015) and especially the human CIP/ VIPS (Orban and Ferri, 2016) as the area for processing object grasping features (Chinellato et al., 2009) including three-dimensional characteristics (Chandrasekaran et al., 2007; Durand et al., 2009; Georgieva et al., 2009; Orban et al., 2006; Rosenberg et al., 2013; Shikata et al., 2001; Shikata et al., 2003; Taira et al., 2001) within the dorsal visual stream. Durand et al. (2009) also demonstrated that the pIPS is involved in processing 3D shapes near grasping-related areas, while Makin et al. (2007) highlighted its role in integrating visual and spatial information in hand-centered coordinates for visuomotor tasks. Our results suggest that the activations observed in the occipital IPS/CIP likely represent an area where spatial attributes such as distance are integrated with other features, including orientation and size of 3D graspable objects, aligning with Chinellato and Del Pobil (2008), to prepare potential hand-object interactions within the PPS, resulting from the top-down perspective.

The activation patterns for objects in PPS and EPS suggest that presentations in PPS elicit activations directed towards a dorsal (or "vision-for-action" (Goodale et al., 1994; Hebart and Hesselmann, 2012)) pathway, involving the lateral components of V3d and central components of V3v, extending to the pIPS/ CIP. In contrast, stimuli in EPS activate the central components of V3d and the lateral areas of V3v, following a more ventral (or "vision-for-perception" (Goodale et al., 1994; Hebart and Hesselmann, 2012) pathway, consistent with prior research (Basile et al., 2024) (see Fig. 4a, b).

Based on the anatomical distinction proposed by Rizzolatti and Matelli (2003), Binkofski and Buxbaum (2013) differentiated two functional pathways within the dorsal stream: the dorso-dorsal stream, primarily involved in the organization of action and control of movements ("Grasp System"), and the ventro-dorsal stream, which integrates spatial and functional attributes of objects to support tool-related knowledge and action preparation. ("Use System"). While some studies suggest that action understanding may involve the ventral stream (Wurm and Caramazza, 2019), the ventro-dorsal pathway remains crucial for linking object affordances with motor actions. Recent findings by Jüchtern et al. (2024) supported a medio-dorsal subpathway, linking the SPL and IPS with premotor cortex (PM), facilitating movement coordination and object manipulation. The processing gradient from dorsal to ventral streams shows a transition from hidden state exploration (actively sampling sensory inputs to infer latent spatial and contextual properties of the environment, reducing uncertainty and enabling goal-directed motor control), surprise-driven attention, and goal-directed motor control in dorsal streams, to symbolic gestures and abstract action aspects in more ventral streams (Goodale and Milner, 1992; Proietti et al., 2023a; Stoll et al., 2024). Our activation patterns of the dorsal stream, including the pIPS/ CIP for stimuli in PPS align with the concept of affordances by Sakreida et al. (2016) and Costantini et al. (2011) and indicate that objects in PPS are primarily processed in the medio-dorsal stream processing, implying movement coordination (Tomassini et al., 2007) and manual object manipulation (Binkofski et al., 1999). While for both, object presentation in EPS and PPS, the analysis and contextualization of the scene, intrinsic object properties, and semantic aspects, primarily processed ventrally (Proietti et al., 2023a; Stoll et al., 2024), may be relevant, stimuli in PPS engage additional dorsal IPS processing due to potential opportunities for interaction.

These findings align additionally with the concept of the "attentional landscape" introduced by Baldauf and Deubel (2010), who propose that attentional resources are dynamically distributed across the visual field depending on the potential relevance for interaction. As shown by Baldauf et al. (2008) the posterior parietal cortex, including the pIPS, may encode multiple potential reach targets in parallel, whereby the graspable nature of our stimuli triggered affordance-based action evaluation and directed attention toward nearby, action-relevant PPS. In contrast, stimuli in EPS recruited ventral stream areas, consistent with attention being directed toward semantic processing and object recognition in less action-relevant space.

Ventral and dorsal components of V3 are activated in response to both stimuli in PPS and EPS, suggesting interconnections between the dorsal and ventral streams. Consistent with this, Van Polanen and Davare (2015) and Milner (2017) propose that the dorsal stream obtains detailed object information from ventral stream areas for "fine-tuned grip adjustments", while the ventral stream may receive grasp-related information from dorsal regions to improve object representation.

Contrary to our predictions, our study did not show activations in areas typically associated with the PPS network, such as PMv and the aIPS (Cléry et al., 2018). This may be due to our stimuli primarily involving spatial perception rather than interaction with objects, potentially explaining the lack of frontal area activation. The absence of significant activation in the anterior IPS, often linked to further 3D perception in PPS in macaques (Durand et al., 2007; Srivastava et al., 2009; Theys et al., 2012) suggests that our 3D presentation might not have been sufficiently immersive. Nevertheless, our results demonstrate clear visual and intraparietal activation patterns that align with previous findings on PPS and EPS processing.

4.2.2. *PPS and EPS processing controlled for pixel size*

Our experimental design incorporates controls for both distance and object size, allowing us to differentiate activations driven by spatial context from those potentially influenced by differences in pixel object size between stimuli in PPS and EPS. When pixel size was held constant (PPS_Small vs EPS_Large), we observed only minor deviations in activation patterns compared to the uncontrolled contrasts (see Fig. 5 and Table 2).

Although the activation patterns for EPS > PPS with controlled pixel size were like those in simple EPS > PPS contrasts, we observed additional activations in a bilateral region. This region could correspond to probabilistic maps of V3v, as seen in the simple EPS > PPS contrast, or V4v. Previous studies indicate that V4v, like V3v, may be involved in encoding the actual size of objects rather than just their pixel image size (Tanaka and Fujita, 2015; Weidner et al., 2014). This supports the idea that recalculating perceived size from distant objects, rather than relying solely on pixel size, is processed within higher visual areas such as V3v or V4v.

4.2.3. *Influence of stereoscopic presentation*

Stereoscopic stimulus presentation elicited significant activation clusters in the ventral and dorsal visual stream primarily along the right pIPS, bilateral Area V5/MT, and LOC (see Fig. 4e). The involvement of the dorsal stream, especially the mediocaudal hIP7 as part of the posterior IPS (Richter et al., 2018) (CIP in primates (Orban, 2016; Shikata et al., 2008)), in processing 3D shape from binocular disparity aligns with previous studies in primates (Kusunoki, 1993; Orban, 2016; Shikata et al., 1996; Taira et al., 2000; Tsutsui et al., 2001; Tsutsui et al., 2002; Van Dromme et al., 2016) and human (Durand et al., 2009; Georgieva et al., 2009; Shikata et al., 2001; Shikata et al., 2003; Taira et al., 2001). This suggests that stereoscopic representation enhanced depth perception, particularly relevant in EPS, with behavioral and self-report data indicating increased immersion and longer response times.

The strong engagement of the pIPS under stereoscopic conditions may reflect also that stereoscopic presentation presents objects more graspable and spatially embedded, thereby increasing their action-

related affordances. This could enhance the relevance of objects for potential upcoming actions especially within peripersonal space where spatial encoding and motor preparation are more tightly coupled.

The right-lateralized pIPS activation supports findings of right hemisphere dominance in stereoscopic depth perception processing (Lohia et al., 2024; Nishida et al., 2001; Shikata et al., 2003; Taira et al., 2001; Wang et al., 2016).

Activations in V5/MT and LOC further support the involvement of both dorsal and ventral visual streams in processing binocular disparity (Goncalves et al., 2015; Parker et al., 2016; Sanada et al., 2012) and extend our understanding of V5/MT's role beyond motion detection to static 3D object perception (Chen et al., 2020; Goncalves et al., 2015; Kourtzi et al., 2002). Furthermore, LOC's contribution to grasp planning indicated by Buchwald et al. (2018) is supported by our results.

4.2.4. *Influence of object size*

Our examination of object size-related activations revealed that large objects elicited responses in LOC (Cohen et al., 1994; Weidner and Fink, 2006; Zeng et al., 2020), V3 (Boussaoud et al., 1990; Konen and Kastner, 2008; Lee and van Donkelaar, 2002), and V4 (Boussaoud et al., 1990; Konen and Kastner, 2008; Lee and van Donkelaar, 2002; Proietti et al., 2023a; Tanaka and Fujita, 2015; Wurm and Caramazza, 2022), consistent with previous findings suggesting their role in processing perceived object size (*see* Fig. 4c). In contrast, smaller objects, activated cognitive control areas belonging to the salience network, such as the Insula (Menon and Uddin, 2010) and the ACC (Kollenburg et al., 2025) (*see* Fig. 4d). Activations in the frontal eye fields (FEF/BA6) and IPS align with previous research identifying these regions as key nodes in the dorsal attention network (DAN) (Corbetta and Shulman, 2002). Small objects increased task difficulty, eliciting prefrontal activations in BA 44/45 (Goghari and MacDonald, 2009; Rubia et al., 2001) and the preSMA (Garavan et al., 1999; Obeso et al., 2013), linked to response inhibition, that is crucial in go/no-go tasks and cognitive control in previous studies. Previous research has also implicated the frontal operculum and the ACC in response inhibition processes (Krams et al., 1998; Rubia et al., 2001). This heightened demand for attention and concentration might also be reflected in significantly longer response times for small stimuli in EPS. Activations in V1 and V2 reflect enhanced visual attention required for smaller objects. In summary we can demonstrate reliable activations associated with variations in object size, although the overlap between distance and object size-controlled distance further validates, that the activations in the dorsal stream were driven by spatial distance rather than being influenced by object size.

4.3. *Limitations*

Although stimulus presentation was pseudorandomized to reduce predictability, the design was not optimized to explicitly model sequential or carry-over effects.

Due to the limited space within the MRI scanner and the necessity of using head coils for imaging, MRI-compatible VR headsets are designed to enclose the eyes in a binocular-like fashion. This design, which includes black borders at the edges of the visual field, restricts the participant's FOV, reducing the sense of presence (IJsselsteijn et al., 2001) and immersion.

Additionally, the requirement for maintain head immobility within the MRI scanner to ensure high-quality imaging may have further reduced the sense of presence (IJsselsteijn et al., 2001) and a less realistic experience of the visual environment. Nevertheless, the MRI-compatible VR video goggle system remains the only and most effective method currently available for presenting virtual scenes during fMRI acquisition.

Moreover, participants were unable to physically interact with the virtual objects, which could have influenced the perceived reachability of stimuli. However, post-session questionnaires confirmed that objects presented in peripersonal space were consistently judged as reachable, and those in extrapersonal space as unreachable.

Further the study did not include eye-tracking, which could have confirmed fixation, gaze stability, and attentional engagement. This is particularly relevant given the fixed 2300 ms stimulus duration, where early responses might have led to premature disengagement. Nonetheless, minimal differences in response times and participants' overall high accuracy suggest that any variability in attentional engagement was negligible and attention was maintained as instructed.

4.4. *Implications for future research*

The primary objective of the present study was to examine whether object presentation in PPS activates potential affordances processed by the dorsal visual stream as part of a PPS network, regardless of object size. We successfully demonstrated that realistic VR object presentations in PPS activates the dorsal visual stream, including the pIPS, related to potential object interaction, whereas presentations in EPS primarily engage ventral visual regions associated with semantic object properties. Activation pattern in V5/MT, LOC and IPS during stereoscopic viewing underscores the potential of VR-fMRI integration for investigating depth perception and spatial processing. These findings have significant implications for clinical cognitive science and neuroimaging methodology, suggesting that VR can enhance the ecological validity of fMRI experiments while maintaining full experimental control of the task.

Future neuroimaging studies could build on this approach by implementing more immersive VR experiences. However, such advancements may necessitate the exploration of alternative neuroimaging methods like functional near-infrared spectroscopy (fNIRS) or mobile electroencephalography (EEG) to accommodate naturalistic body movements. Using fNIRS, one could not only overcome the physical constraints of MRI but also implement interactive paradigms involving motion-tracking of hands, thereby allowing the investigation of body-related spatial processing. For instance, Makin et al. (2007) demonstrated that visual areas exhibit hand-centered representations when stimuli are presented near the body, indicating visually dominant perihand encoding. Similarly, Pamplona et al. (2024) showed that changes in the visual availability of a virtual hand modulate neural activity in both visual and body-related cortical areas, emphasizing that the nature of the stimulus, especially its bodily relevance, shapes the spatial reference frames engaged. Future work could benefit from systematically contrasting object- versus body-related stimuli, to further analyze whether observed effects are driven by spatial proximity alone or by the embodied salience of the stimuli.

Future fNIRS-based setups could also be combined with mixed reality environments, which allow for the merging of real-world environments with virtual stimuli to incorporate tactile and proprioceptive inputs, providing spatial processing under more naturalistic, multisensory conditions. VR-fMRI integration and potential fNIRS setups could support the development of more effective VR-based interventions in clinical applications, particularly in rehabilitation (Chen et al., 2018; de Rooij et al., 2016), Apraxia (Binkofski et al., 2003) and exposure therapy (Kim and Kim, 2020; Van Loenen et al., 2022; Wechsler et al., 2019).

CRediT authorship contribution statement

Meret Mertens: Writing – review & editing, Writing – original draft, Visualization, Resources, Methodology, Investigation, Formal analysis, Data curation. **Ferdinand Binkofski:** Supervision, Project administration, Funding acquisition, Conceptualization. **Bruno Leitão:** Methodology. **Bichr Grii:** Methodology. **Rea Rodriguez-Raecke:** Resources, Project administration, Conceptualization. **André Schüppen:** Investigation. **Antonello Pellicano:** Conceptualization. **Lukas Lorentz:** Writing – review & editing, Supervision, Formal analysis. **Rik Sijben:** Writing – review & editing, Validation, Supervision, Project

administration, Methodology, Formal analysis.

Declaration of competing interest

The authors declare that they have no known competing financial interests or personal relationships that could have appeared to influence the work reported in this article.

Acknowledgements

This work was supported by *the Brain Imaging Facility of the Interdisciplinary Centre for Clinical Research (IZKF) Aachen* within the Faculty of Medicine at RWTH Aachen University. Special acknowledgments appertain to Oleg Poznansky for adjusting the scanning sequences and the pre-processing pipeline and Harshal Patel for his support in conducting the MRI measurements. We would like to thank all participants in this study.

This study was funded by Interreg North-West Europe within the framework of the "Scale-Up4Rehab" project (NWE0100082) dedicated to the research and development of Virtual Reality technology in the healthcare sector.

Data availability

Scripts used to run the object perception task, along with all necessary data, stimulus images as well as behavioral data presented in Figure 3, are available on the Open Science Framework (https://osf.io/4s6q7/). In adherence to ethical restrictions, additional data is available upon reasonable request.

References

Anderson, J.C., Martin, K.A.C., 2009. The synaptic connections between cortical areas V1 and V2 in Macaque Monkey. J. Neurosci. 29 (36), 11283–11293. https://doi.org/10.1523/jneurosci.5757-08.2009.

Baldauf, D., Cui, H., Andersen, R.A., 2008. The posterior parietal cortex encodes in parallel both goals for double-reach sequences. J. Neurosci. 28 (40), 10081–10089. https://doi.org/10.1523/jneurosci.3423-08.2008.

Baldauf, D., Deubel, H., 2010. Attentional landscapes in reaching and grasping. Vis. Res. 50 (11), 999–1013. https://doi.org/10.1016/j.visres.2010.02.008.

Basile, G.A., Tatti, E., Bertino, S., Milardi, D., Genovese, G., Bruno, A., Muscatello, M.R. A., Ciurleo, R., Cerasa, A., Quartarone, A., Cacciola, A., 2024. Neuroanatomical correlates of peripersonal space: bridging the gap between perception, action, emotion and social cognition. Brain Struct. Funct. 229 (5), 1047–1072. https://doi.org/10.1007/s00429-024-02781-9.

Berryhill, M., Olson, I.R., 2009. The representation of object distance: evidence from neuroimaging and neuropsychology [Original research]. Front. Hum. Neurosci. 3. https://doi.org/10.3389/neuro.09.043.2009.

Beschin, N., Robertson, I.H., 1997. Personal versus extrapersonal neglect: a group study of their dissociation using a reliable clinical test. Cortex 33 (2), 379–384. https://doi.org/10.1016/s0010-9452(08)70013-3.

Binkofski, F., Buccino, G., Stephan, K.M., Rizzolatti, G., Seitz, R.J., Freund, H.J., 1999. A parieto-premotor network for object manipulation: evidence from neuroimaging. Exp. Brain Res. 128 (1–2), 210–213. https://doi.org/10.1007/s002210050838.

Binkofski, F., Butler, A., Buccino, G., Heide, W., Fink, G., Freund, H.J., Seitz, R.J., 2003. Mirror apraxia affects the peripersonal mirror space. A combined lesion and cerebral activation study. Exp. Brain Res. 153 (2), 210–219. https://doi.org/10.1007/s00221-003-1594-2.

Binkofski, F., Buxbaum, L.J., 2013. Two action systems in the human brain. Brain Lang. 127 (2), 222–229. https://doi.org/10.1016/j.bandl.2012.07.007.

Blanca, M.J., Alarcón, R., Arnau, J., Bono, R., Bendayan, R., 2017. Non-normal data: is ANOVA still a valid option? Psicothema 29 (4), 552–557. https://doi.org/10.7334/psicothema2016.383.

Blini, E., Desoche, C., Salemme, R., Kabil, A., Hadj-Bouziane, F., Farnè, A., 2018. Mind the depth: visual perception of shapes is better in peripersonal space. Psychol. Sci. 29 (11), 1868–1877. https://doi.org/10.1177/0956797618795679.

Bogdanova, O.V., Bogdanov, V.B., Dureux, A., Farnè, A., Hadj-Bouziane, F., 2021. The Peripersonal Space in a social world. Cortex 142, 28–46. https://doi.org/10.1016/j.cortex.2021.05.005.

Boussaoud, D., Ungerleider, L.G., Desimone, R., 1990. Pathways for motion analysis: cortical connections of the medial superior temporal and fundus of the superior temporal visual areas in the macaque. J. Comp. Neurol. 296 (3), 462–495. https://doi.org/10.1002/cne.902960311.

Brozzoli, C., Makin, T.R., Cardinali, L., Holmes, N.P., Farnè, A., 2012. Peripersonal space: a multisensory interface for body–object interactions. In: Murray, M.M., Wallace, M. T. (Eds.), The Neural Bases of Multisensory Processes. CRC Press/Taylor & Francis. https://centaur.reading.ac.uk/23376/.

Buchwald, M., Przybylski, Ł., Króliczak, G., 2018. Decoding brain states for planning functional grasps of tools: a functional magnetic resonance imaging multivoxel pattern analysis study. J. Int. Neuropsychol. Soc. 24 (10), 1013–1025. https://doi.org/10.1017/s1355617718000590.

Cartaud, A., Ruggiero, G., Ott, L., Iachini, T., Coello, Y., 2018. Physiological response to facial expressions in peripersonal space determines interpersonal distance in a social interaction context. Front. Psychol. 9, 657. https://doi.org/10.3389/fpsyg.2018.00657.

Chandrasekaran, C., Canon, V., Dahmen, J.C., Kourtzi, Z., Welchman, A.E., 2007. Neural correlates of disparity-defined shape discrimination in the human brain. J. Neurophysiol. 97 (2), 1553–1565. https://doi.org/10.1152/jn.01074.2006.

Chen, N., Chen, Z., Fang, F., 2020. Functional specialization in human dorsal pathway for stereoscopic depth processing. Exp. Brain Res. 238 (11), 2581–2588. https://doi.org/10.1007/s00221-020-05918-4.

Chen, Y., Fanchiang, H.D., Howard, A., 2018. Effectiveness of virtual reality in children with cerebral palsy: a systematic review and meta-analysis of randomized controlled trials. Phys. Ther. 98 (1), 63–77. https://doi.org/10.1093/ptj/pzx107.

Chinellato, E., & Del Pobil, A.P. (2008). Neural coding in the dorsal visual stream. In M. Asada, J. C. T. Hallam, J.A. Meyer, & J. Tani, From Animals to Animats 10 Berlin, Heidelberg.

Chinellato, E., Grzyb, B.J., Fattori, P., Del Pobil, A.P., 2009. Toward an integrated visuomotor representation of the peripersonal space. In: Proceedings of the Bioinspired Applications in Artificial and Natural Computation: Third International Work-Conference on the Interplay Between Natural and Artificial Computation, IWINAC 2009. Santiago de Compostela, Spain. June 22-26, 2009, Proceedings, Part II 3.

Cho, H., Kang, M.-K., Ahn, S., Kwon, M., Yoon, K.-J., Kim, K., Jun, S.C., 2016. Cortical responses and shape complexity of stereoscopic image - a simultaneous EEG/MEG study. Neurosignals 24 (1), 102–112. https://doi.org/10.1159/000442617.

Cléry, J., Guipponi, O., Odouard, S., Wardak, C., Ben Hamed, S., 2018. Cortical networks for encoding near and far space in the non-human primate. Neuroimage 176, 164–178. https://doi.org/10.1016/j.neuroimage.2018.04.036.

Cléry, J., Guipponi, O., Wardak, C., Ben Hamed, S., 2015. Neuronal bases of peripersonal and extrapersonal spaces, their plasticity and their dynamics: knowns and unknowns. Neuropsychologia 70, 313–326. https://doi.org/10.1016/j.neuropsychologia.2014.10.022.

Cohen, L., Gray, F., Meyrignac, C., Dehaene, S., Degos, J.D., 1994. Selective deficit of visual size perception: two cases of hemimicropsia. J. Neurol. Neurosurg. Psychiatry 57 (1), 73–78. https://doi.org/10.1136/jnnp.57.1.73.

Corbetta, M., Shulman, G.L., 2002. Control of goal-directed and stimulus-driven attention in the brain. Nat. Rev. Neurosci. 3 (3), 201–215. https://doi.org/10.1038/nrn755.

Costantini, M., Ambrosini, E., Scorolli, C., Borghi, A.M., 2011. When objects are close to me: affordances in the peripersonal space. Psychon. Bull. Rev. 18 (2), 302–308. https://doi.org/10.3758/s13423-011-0054-4.

de Borst, A.W., de Gelder, B., 2022. Threat detection in nearby space mobilizes human ventral premotor cortex, intraparietal sulcus, and amygdala. Brain Sci. 12 (3), 391. https://www.mdpi.com/2076-3425/12/3/391.

de Rooij, I.J.M., van de Port, I.G.L., Meijer, J.W.G., 2016. Effect of virtual reality training on balance and gait ability in patients with stroke: systematic review and meta-analysis. Phys. Ther. 96 (12), 1905–1918. https://doi.org/10.2522/ptj.20160054.

Durand, J.B., Nelissen, K., Joly, O., Wardak, C., Todd, J.T., Norman, J.F., Janssen, P., Vanduffel, W., Orban, G.A., 2007. Anterior regions of monkey parietal cortex process visual 3D shape. Neuron 55 (3), 493–505. https://doi.org/10.1016/j.neuron.2007.06.040.

Durand, J.B., Peeters, R., Norman, J.F., Todd, J.T., Orban, G.A., 2009. Parietal regions processing visual 3D shape extracted from disparity. Neuroimage 46 (4), 1114–1126. https://doi.org/10.1016/j.neuroimage.2009.03.023.

Ellena, G., Bertoni, T., Durand-Ruel, M., Thoresen, J., Sandi, C., Serino, A., 2022. Acute stress affects peripersonal space representation in cortisol stress responders. Psychoneuroendocrinology 142, 105790. https://doi.org/10.1016/j.psyneuen.2022.105790.

Fang, F., Boyaci, H., Kersten, D., Murray, S.O., 2008. Attention-dependent representation of a size illusion in human V1. Curr. Biol. 18 (21), 1707–1712. https://doi.org/10.1016/j.cub.2008.09.025.

Farnè, I., Làdavas, 2005. Shaping multisensory action-space with tools: evidence from patients with cross-modal extinction. Neuropsychologia 43 (2), 238–248. https://doi.org/10.1016/j.neuropsychologia.2004.11.010.

Farnè, Làdavas, 2000. Dynamic size-change of hand peripersonal space following tool use. Neuroreport 11 (8), 1645–1649. https://journals.lww.com/neuroreport/fulltext/2000/06050/dynamic_size_change_of_hand_peripersonal_space.10.aspx.

Fossataro, C., Sambo, C.F., Garbarini, F., Iannetti, G.D., 2016. Interpersonal interactions and empathy modulate perception of threat and defensive responses. Sci. Rep. 6 (1), 19353. https://doi.org/10.1038/srep19353.

Garavan, H., Ross, T.J., Stein, E.A., 1999. Right hemispheric dominance of inhibitory control: an event-related functional MRI study. Proc. Natl. Acad. Sci. USA 96 (14), 8301–8306. https://doi.org/10.1073/pnas.96.14.8301.

Gattass, R., Sousa, A., Gross, C., 1988. Visuotopic organization and extent of V3 and V4 of the macaque. J. Neurosci. 8 (6), 1831–1845. https://doi.org/10.1523/jneurosci.08-06-01831.1988.

Georgieva, S., Peeters, R., Kolster, H., Todd, J.T., Orban, G.A., 2009. The processing of three-dimensional shape from disparity in the human brain. J. Neurosci. 29 (3), 727–742. https://doi.org/10.1523/jneurosci.4753-08.2009.

Goghari, V.M., MacDonald, A.W., 2009. The neural basis of cognitive control: response selection and inhibition. Brain Cogn. 71 (2), 72–83. https://doi.org/10.1016/j.bandc.2009.04.004.

Goncalves, N.R., Ban, H., Sánchez-Panchuelo, R.M., Francis, S.T., Schluppeck, D., Welchman, A.E., 2015. 7 Tesla fMRI reveals systematic functional organization for binocular disparity in dorsal visual cortex. J. Neurosci. 35 (7), 3056–3072. https://doi.org/10.1523/jneurosci.3047-14.2015.

Goodale, M.A., Meenan, J.P., Bülthoff, H.H., Nicolle, D.A., Murphy, K.J., Racicot, C.I., 1994. Separate neural pathways for the visual analysis of object shape in perception and prehension. Curr. Biol. 4 (7), 604–610. https://doi.org/10.1016/S0960-9822(00)00132-9.

Goodale, M.A., Milner, A.D., 1992. Separate visual pathways for perception and action. Trends Neurosci. 15 (1), 20–25. https://doi.org/10.1016/0166-2236(92)90344-8.

Gori, M., Sciutti, A., Burr, D., Sandini, G., 2011. Direct and indirect haptic calibration of visual size judgments. PLoS ONE 6 (10), e25599. https://doi.org/10.1371/journal.pone.0025599.

Graziano, M.S.A., Cooke, D.F., 2006. Parieto-frontal interactions, personal space, and defensive behavior. Neuropsychologia 44 (6), 845–859. https://doi.org/10.1016/j.neuropsychologia.2005.09.009.

Grivaz, P., Blanke, O., Serino, A., 2017. Common and distinct brain regions processing multisensory bodily signals for peripersonal space and body ownership. Neuroimage 147, 602–618. https://doi.org/10.1016/j.neuroimage.2016.12.052.

Gruber, H.E., 1954. The relation of perceived size to perceived distance. Am. J. Psychol. 67 (3), 411–426. https://doi.org/10.2307/1417933.

Hebart, M.N., Hesselmann, G., 2012. What visual information is processed in the human dorsal stream? J. Neurosci. 32 (24), 8107–8109. https://doi.org/10.1523/jneurosci.1462-12.2012.

Heed, T., Habets, B., Sebanz, N., Knoblich, G., 2010. Others' actions reduce crossmodal integration in peripersonal space. Curr. Biol. 20 (15), 1345–1349. https://doi.org/10.1016/j.cub.2010.05.068.

Higashiyama, A., Shimono, K., 2004. Mirror vision: perceived size and perceived distance of virtual images. Percept. Psychophys. 66 (4), 679–691. https://doi.org/10.3758/BF03194911.

Holway, A.H., Boring, E.G., 1941. Determinants of apparent visual size with distance variant. Am. J. Psychol. 54 (1), 21–37. https://doi.org/10.2307/1417790.

Horváth, G., Nemes, V.A., Radó, J., Czigler, A., Török, B., Buzás, P., Jandó, G., 2018. Correction: simple reaction times to cyclopean stimuli reveal that the binocular system is tuned to react faster to near than to far objects. PLoS ONE 13 (8), e0202358. https://doi.org/10.1371/journal.pone.0202358.

IJsselsteijn, R., Freeman, A., Bouwhuis, 2001. Effects of stereoscopic presentation, image motion, and screen size on subjective and objective corroborative measures of presence. Presence 10 (3), 298–311. https://doi.org/10.1162/105474601300343621.

Jüchtern, M., Shaikh, U.J., Caspers, S., Binkofski, F., 2024. A gradient of hemisphere-specific dorsal to ventral processing routes in parieto-premotor networks. Netw. Neurosci. 8 (4), 1563–1589. https://doi.org/10.1162/netn_a_00407.

Kaas, J.H., Roe, A.W., Baldwin, M.K.L., Lyon, D.C., 2015. Resolving the organization of the territory of the third visual area: a new proposal. Vis. Neurosci. 32, E016. https://doi.org/10.1017/S0952523815000152.

Kilpatrick, F.P., Ittelson, W.H., 1953. The size-distance invariance hypothesis. Psychol. Rev. 60 (4), 223–231. https://doi.org/10.1037/h0060882.

Kim, S., Kim, E., 2020. The use of virtual reality in psychiatry: a review. J. Korean Acad. Child Adolesc. Psychiatry 31 (1), 26–32. https://doi.org/10.5765/jkacap.190037.

Kollenburg, L., Arnts, H., Green, A., Strauss, I., Vinke, S., Kurt, E., 2025. The cingulum: anatomy, connectivity and what goes beyond. Brain Commun. https://doi.org/10.1093/braincomms/fcaf048.

Konen, C.S., Kastner, S., 2008. Two hierarchically organized neural systems for object information in human visual cortex. Nat. Neurosci. 11 (2), 224–231. https://doi.org/10.1038/nn2036.

Kourtzi, Z., Bülthoff, H.H., Erb, M., Grodd, W., 2002. Object-selective responses in the human motion area MT/MST. Nat. Neurosci. 5 (1), 17–18. https://doi.org/10.1038/nn780.

Krams, M., Rushworth, M.F., Deiber, M.P., Frackowiak, R.S., Passingham, R.E., 1998. The preparation, execution and suppression of copied movements in the human brain. Exp. Brain Res. 120 (3), 386–398. https://doi.org/10.1007/s002210050412.

Kusunoki, M., 1993. Selectivity of the parietal visual neurons in the axis orientation of objects in space. Soc. Nurosci. Abstr. 19, 770. https://cir.nii.ac.jp/crid/1570854174684277504.

Lee, J.H., van Donkelaar, P., 2002. Dorsal and ventral visual stream contributions to perception-action interactions during pointing. Exp. Brain Res. 143 (4), 440–446. https://doi.org/10.1007/s00221-002-1011-2.

Lohia, K., Soans, R.S., Saxena, R., Mahajan, K., Gandhi, T.K., 2024. Distinct rich and diverse clubs regulate coarse and fine binocular disparity processing: evidence from stereoscopic task-based fMRI. iScience 27 (6). https://doi.org/10.1016/j.isci.2024.109831.

Lorentz, L., Schüppen, A., Suchan, B., Binkofski, F., 2023. Neural correlates of virtual reality-based attention training: an fMRI study. Neuroimage 284, 120454. https://doi.org/10.1016/j.neuroimage.2023.120454.

Makin, T.R., Holmes, N.P., Zohary, E., 2007. Is that near my hand? Multisensory representation of peripersonal space in human intraparietal sulcus. J. Neurosci. 27 (4), 731–740. https://doi.org/10.1523/jneurosci.3653-06.2007.

Malach, R., Levy, I., Hasson, U., 2002. The topography of high-order human object areas. Trends Cogn. Sci. 6 (4), 176–184. https://doi.org/10.1016/S1364-6613(02)01870-3.

McIntire, J., Havig, P., Geiselman, E., 2012. What is 3D Good For? A review of Human Performance on Stereoscopic 3D Displays (Vol. 8383). SPIE. https://doi.org/10.1117/12.920017.

Menon, V., Uddin, L.Q., 2010. Saliency, switching, attention and control: a network model of insula function. Brain Struct. Funct. 214 (5), 655–667. https://doi.org/10.1007/s00429-010-0262-0.

Milner, A.D., 2017. How do the two visual streams interact with each other? Exp. Brain Res. 235 (5), 1297–1308. https://doi.org/10.1007/s00221-017-4917-4.

Mishkin, M., Ungerleider, L.G., Macko, K.A., 1983. Object vision and spatial vision: two cortical pathways. Trends Neurosci. 6, 414–417. https://doi.org/10.1016/0166-2236(83)90190-X.

Murray, S.O., Boyaci, H., Kersten, D., 2006. The representation of perceived angular size in human primary visual cortex. Nat. Neurosci. 9 (3), 429–434. https://doi.org/10.1038/nn1641.

Nishida, Y., Hayashi, O., Iwami, T., Kimura, M., Kani, K., Ito, R., Shiino, A., Suzuki, M., 2001. Stereopsis-processing regions in the human parieto-occipital cortex. Neuroreport 12 (10), 2259–2263. https://doi.org/10.1097/00001756-200107200-00043.

Obeso, I., Robles, N., Muñoz-Marrón, E., Redolar-Ripoll, D., 2013. Dissociating the role of the pre-SMA in response inhibition and switching: a combined online and offline TMS approach [Original Research]. Front. Hum. Neurosci. 7. https://doi.org/10.3389/fnhum.2013.00150.

Orban, G.A., 2016. Functional definitions of parietal areas in human and non-human primates. Proc. R. Soc. B Biol. Sci. 283 (1828), 20160118. https://doi.org/10.1098/rspb.2016.0118.

Orban, G.A., Claeys, K., Nelissen, K., Smans, R., Sunaert, S., Todd, J.T., Wardak, C., Durand, J.B., Vanduffel, W., 2006. Mapping the parietal cortex of human and non-human primates. Neuropsychologia 44 (13), 2647–2667. https://doi.org/10.1016/j.neuropsychologia.2005.11.001.

Orban, G.A., Ferri, S., 2016. Functional Imaging of the Human Visual System. In: Filippi, M. (Ed.), fMRI Techniques and Protocols. Springer, New York, pp. 545–572. https://doi.org/10.1007/978-1-4939-5611-1_18.

Pamplona, G.S.P., Giussani, A., Salzmann, L., Staempfli, P., Schneller, S., Gassert, R., Ionta, S., 2024. Neuro-cognitive effects of degraded visibility on illusory body ownership. Neuroimage 300, 120870. https://doi.org/10.1016/j.neuroimage.2024.120870.

Parker, A.J., Smith, J.E., Krug, K., 2016. Neural architectures for stereo vision. Philos. Trans. R. Soc. Lond. B Biol. Sci. 371 (1697). https://doi.org/10.1098/rstb.2015.0261.

Peirce, J., Gray, J.R., Simpson, S., MacAskill, M., Höchenberger, R., Sogo, H., Kastman, E., Lindeløv, J.K., 2019. PsychoPy2: experiments in behavior made easy. Behav. Res. Methods 51 (1), 195–203. https://doi.org/10.3758/s13428-018-01193-y.

Pellencin, E., Paladino, M.P., Herbelin, B., Serino, A., 2018. Social perception of others shapes one's own multisensory peripersonal space. Cortex 104, 163–179. https://doi.org/10.1016/j.cortex.2017.08.033.

Pitcher, D., Ungerleider, L.G., 2021. Evidence for a third visual pathway specialized for social perception. Trends Cogn. Sci. 25 (2), 100–110. https://doi.org/10.1016/j.tics.2020.11.006.

Plewan, T., Weidner, R., Fink, G.R., 2012. The influence of stimulus duration on visual illusions and simple reaction time. Exp. Brain Res. 223 (3), 367–375. https://doi.org/10.1007/s00221-012-3265-7.

Previc, F.H., 1998. The neuropsychology of 3-D space. Psychol. Bull. 124 (2), 123–164. https://doi.org/10.1037/0033-2909.124.2.123.

Proietti, P., Tessari, 2023a. An active inference model of hierarchical action understanding, learning and imitation. Phys. Life Rev. 46, 92–118. https://doi.org/10.1016/j.plrev.2023.05.012.

Proietti, P., & Tessari. (2023b). Limb apraxia and active inference in the visuomotor pathways.

Richter, M., Amunts, K., Mohlberg, H., Bludau, S., Eickhoff, S.B., Zilles, K., Caspers, S., 2018. Cytoarchitectonic segregation of human posterior intraparietal and adjacent parieto-occipital sulcus and its relation to visuomotor and cognitive functions. Cereb. Cortex 29 (3), 1305–1327. https://doi.org/10.1093/cercor/bhy245.

Riesenhuber, M., Poggio, T., 2000. Models of object recognition. Nat. Neurosci. 3 (11), 1199–1204. https://doi.org/10.1038/81479.

Rizzolatti, G., Fadiga, L., Fogassi, L., Gallese, V., 1997. The space around us. Science 277 (5323), 190–191. https://doi.org/10.1126/science.277.5323.190.

Rizzolatti, G., Matelli, M., 2003. Two different streams form the dorsal visual system: anatomy and functions. Exp. Brain Res. 153 (2), 146–157. https://doi.org/10.1007/s00221-003-1588-0.

Rizzolatti, G., Matelli, M., Pavesi, G., 1983. Deficits in attention and movement following the removal of postarcuate (area 6) and prearcuate (area 8) cortex in macaque monkeys. Brain 106 (Pt 3), 655–673. https://doi.org/10.1093/brain/106.3.655.

Rosenberg, A., Cowan, N.J., Angelaki, D.E., 2013. The visual representation of 3D object orientation in parietal cortex. J. Neurosci. 33 (49), 19352–19361. https://doi.org/10.1523/jneurosci.3174-13.2013.

Rößing, C., Hanika, J., Lensch, H., 2012. Real-time disparity map-based pictorial depth cue enhancement. Comput. Graph. Forum 31 (2pt1), 275–284. https://doi.org/10.1111/j.1467-8659.2012.03006.x.

Rubia, K., Russell, T., Overmeyer, S., Brammer, M.J., Bullmore, E.T., Sharma, T., Simmons, A., Williams, S.C.R., Giampietro, V., Andrew, C.M., Taylor, E., 2001. Mapping motor inhibition: conjunctive brain activations across different versions of Go/No-Go and stop tasks. Neuroimage 13 (2), 250–261. https://doi.org/10.1006/nimg.2000.0685.

Ruggiero, G., Frassinetti, F., Coello, Y., Rapuano, M., di Cola, A.S., Iachini, T., 2017. The effect of facial expressions on peripersonal and interpersonal spaces. Psychol. Res. 81 (6), 1232–1240. https://doi.org/10.1007/s00426-016-0806-x.

Sakreida, K., Effnert, I., Thill, S., Menz, M.M., Jirak, D., Eickhoff, C.R., Ziemke, T., Eickhoff, S.B., Borghi, A.M., Binkofski, F., 2016. Affordance processing in segregated parieto-frontal dorsal stream sub-pathways. Neurosci. Biobehav. Rev. 69, 89–112. https://doi.org/10.1016/j.neubiorev.2016.07.032.

Sanada, T.M., Nguyenkim, J.D., DeAngelis, G.C., 2012. Representation of 3-D surface orientation by velocity and disparity gradient cues in area MT. J. Neurophysiol. 107 (8), 2109–2122. https://doi.org/10.1152/jn.00578.2011.

Schmider, E., Ziegler, M., Danay, E., Beyer, L., Bühner, M., 2010. Is it really robust? Methodology 6 (4), 147–151. https://doi.org/10.1027/1614-2241/a000016.

Serino, A., 2019. Peripersonal space (PPS) as a multisensory interface between the individual and the environment, defining the space of the self. Neurosci. Biobehav. Rev. 99, 138–159. https://doi.org/10.1016/j.neubiorev.2019.01.016.

Serino, A., Noel, J.P., Galli, G., Canzoneri, E., Marmaroli, P., Lissek, H., Blanke, O., 2015. Body part-centered and full body-centered peripersonal space representations. Sci. Rep. 5, 18603. https://doi.org/10.1038/srep18603.

Shikata, Hamzei, F., Glauche, V., Knab, R., Dettmers, C., Weiller, C., Büchel, C., 2001. Surface orientation discrimination activates caudal and anterior intraparietal sulcus in humans: an event-related fMRI study. J. Neurophysiol. 85 (3), 1309–1314. https://doi.org/10.1152/jn.2001.85.3.1309.

Shikata, Hamzei, F., Glauche, V., Koch, M., Weiller, C., Binkofski, F., Büchel, C., 2003. Functional properties and interaction of the anterior and posterior intraparietal areas in humans. Eur. J. Neurosci. 17 (5), 1105–1110. https://doi.org/10.1046/j.1460-9568.2003.02540.x.

Shikata, E., McNamara, A., Sprenger, A., Hamzei, F., Glauche, V., Büchel, C., Binkofski, F., 2008. Localization of human intraparietal areas AIP, CIP, and LIP using surface orientation and saccadic eye movement tasks. Hum. Brain Mapp. 29 (4), 411–421. https://doi.org/10.1002/hbm.20396.

Shikata, E., Tanaka, Y., Nakamura, H., Taira, M., Sakata, H., 1996. Selectivity of the parietal visual neurones in 3D orientation of surface of stereoscopic stimuli. Neuroreport 7 (14), 2389–2394. https://journals.lww.com/neuroreport/fulltext/1996/10020/selectivity_of_the_parietal_visual_neurones_in_3d.22.aspx.

Sperandio, I., Chouinard, P.A., Goodale, M.A., 2012. Retinotopic activity in V1 reflects the perceived and not the retinal size of an afterimage. Nat. Neurosci. 15 (4), 540–542. https://doi.org/10.1038/nn.3069.

Srivastava, S., Orban, G.A., De Mazière, P.A., Janssen, P., 2009. A distinct representation of three-dimensional shape in macaque anterior intraparietal area: fast, metric, and coarse. J. Neurosci. 29 (34), 10613–10626. https://doi.org/10.1523/jneurosci.6016-08.2009.

Stoll, S., Lorentz, L., Binkofski, F., Randerath, J., 2024. Apraxia: from neuroanatomical pathways to clinical manifestations. Curr. Neurol. Neurosci. Rep. 25 (1), 1. https://doi.org/10.1007/s11910-024-01391-6.

Stone, K.D., Kandula, M., Keizer, A., Dijkerman, H.C., 2018. Peripersonal space boundaries around the lower limbs. Exp. Brain Res. 236 (1), 161–173. https://doi.org/10.1007/s00221-017-5115-0.

Taira, M., Nose, I., Inoue, K., Tsutsui, K.I., 2001. Cortical areas related to attention to 3D surface structures based on shading: an fMRI study. Neuroimage 14 (5), 959–966. https://doi.org/10.1006/nimg.2001.0895.

Taira, M., Tsutsui, K.I., Jiang, M., Yara, K., Sakata, H., 2000. Parietal Neurons Represent Surface Orientation From the Gradient of Binocular Disparity. J. Neurophysiol. 83 (5), 3140–3146. https://doi.org/10.1152/jn.2000.83.5.3140.

Tanaka, S., Fujita, I., 2015. Computation of object size in visual cortical area V4 as a neural basis for size constancy. J. Neurosci. 35 (34), 12033–12046. https://doi.org/10.1523/jneurosci.2665-14.2015.

Theys, T., Srivastava, S., van Loon, J., Goffin, J., Janssen, P., 2012. Selectivity for three-dimensional contours and surfaces in the anterior intraparietal area. J. Neurophysiol. 107 (3), 995–1008. https://doi.org/10.1152/jn.00248.2011.

Tomassini, V., Jbabdi, S., Klein, J.C., Behrens, T.E., Pozzilli, C., Matthews, P.M., Rushworth, M.F., Johansen-Berg, H., 2007. Diffusion-weighted imaging tractography-based parcellation of the human lateral premotor cortex identifies dorsal and ventral subregions with anatomical and functional specializations. J. Neurosci. 27 (38), 10259–10269. https://doi.org/10.1523/jneurosci.2144-07.2007.

Tsutsui, K.I., Jiang, M., Yara, K., Sakata, H., Taira, M., 2001. Integration of perspective and disparity cues in surface-orientation–selective neurons of area CIP. J. Neurophysiol. 86 (6), 2856–2867. https://doi.org/10.1152/jn.2001.86.6.2856.

Tsutsui, K.I., Sakata, H., Naganuma, T., Taira, M., 2002. Neural correlates for perception of 3D surface orientation from texture gradient. Science 298 (5592), 409–412. https://doi.org/10.1126/science.1074128.

Van Dromme, I.C., Premereur, E., Verhoef, B.E., Vanduffel, W., Janssen, P., 2016. Posterior parietal cortex drives inferotemporal activations during three-dimensional object vision. PLoS Biol. 14 (4), e1002445. https://doi.org/10.1371/journal.pbio.1002445.

Van Loenen, I., Scholten, W., Muntingh, A., Smit, J., Batelaan, N., 2022. The effectiveness of virtual reality exposure-based cognitive behavioral therapy for severe anxiety disorders, obsessive-compulsive disorder, and posttraumatic stress disorder: meta-analysis. J. Med. Internet Res. 24 (2), e26736. https://doi.org/10.2196/26736.

Van Polanen, V., Davare, M., 2015. Interactions between dorsal and ventral streams for controlling skilled grasp. Neuropsychologia 79, 186–191. https://doi.org/10.1016/j.neuropsychologia.2015.07.010.

Vieira, J.B., Pierzchajlo, S.R., Mitchell, D.G.V., 2020. Neural correlates of social and non-social personal space intrusions: role of defensive and peripersonal space systems in interpersonal distance regulation. Soc. Neurosci. 15 (1), 36–51. https://doi.org/10.1080/17470919.2019.1626763.

Waldow, K., Decker, L., Mišiak, M., Fuhrmann, A., Roth, D., Latoschik, M.E., 2024. Investigating incoherent depth perception features in virtual reality using stereoscopic impostor-based rendering. In: Proceedings of the IEEE Conference on Virtual Reality and 3D User Interfaces Abstracts and Workshops (VRW).

Wang, A., Li, Y., Zhang, M., Chen, Q., 2016. The role of parieto-occipital junction in the interaction between dorsal and ventral streams in disparity-defined near and far space processing. PLoS ONE 11 (3), e0151838. https://doi.org/10.1371/journal.pone.0151838.

Wechsler, T.F., Kümpers, F., Mühlberger, A., 2019. Inferiority or even superiority of virtual reality exposure therapy in phobias?–A systematic review and quantitative meta-analysis on randomized controlled trials specifically comparing the efficacy of virtual reality exposure to gold standard *in vivo* exposure in agoraphobia, specific phobia, and social phobia [Systematic review]. Front. Psychol. 10. https://doi.org/10.3389/fpsyg.2019.01758.

Weidner, R., Fink, G.R., 2006. The neural mechanisms underlying the müller-lyer illusion and its interaction with visuospatial judgments. Cereb. Cortex 17 (4), 878–884. https://doi.org/10.1093/cercor/bhk042.

Weidner, R., Plewan, T., Chen, Q., Buchner, A., Weiss, P.H., Fink, G.R., 2014. The moon illusion and size–distance scaling–evidence for shared neural patterns. J. Cogn. Neurosci. 26 (8), 1871–1882. https://doi.org/10.1162/jocn_a_00590.

Wurm, M.F., Caramazza, A., 2019. Distinct roles of temporal and frontoparietal cortex in representing actions across vision and language. Nat. Commun. 10 (1), 289. https://doi.org/10.1038/s41467-018-08084-y.

Wurm, M.F., Caramazza, A., 2022. Two 'what' pathways for action and object recognition. Trends Cogn. Sci. 26 (2), 103–116. https://doi.org/10.1016/j.tics.2021.10.003.

Zeng, H., Fink, G.R., Weidner, R., 2020. Visual size processing in early visual cortex follows lateral occipital cortex involvement. J. Neurosci. 40 (22), 4410–4417. https://doi.org/10.1523/jneurosci.2437-19.2020.